RESEARCH ARTICLE

National Science Review
9: nwab011, 2022
https://doi.org/10.1093/nsr/nwab011
Advance access publication 21 January 2021

PHYSICS

Experimental exploration of five-qubit quantum error-correcting code with superconducting qubits

Ming Gong[1,2,3,†], Xiao Yuan[1,2,4,5,†], Shiyu Wang[1,2,3], Yulin Wu[1,2,3], Youwei Zhao[1,2,3], Chen Zha[1,2,3], Shaowei Li[1,2,3], Zhen Zhang[4], Qi Zhao[4], Yunchao Liu[4], Futian Liang[1,2,3], Jin Lin[1,2,3], Yu Xu[1,2,3], Hui Deng[1,2,3], Hao Rong[1,2,3], He Lu[1,2], Simon C. Benjamin[5], Cheng-Zhi Peng[1,2,3], Xiongfeng Ma[4,*], Yu-Ao Chen[1,2,3,*], Xiaobo Zhu[1,2,3,*] and Jian-Wei Pan[1,2,3,*]

[1]Hefei National Laboratory for Physical Sciences at the Microscale and Department of Modern Physics, University of Science and Technology of China, Hefei 230026, China; [2]Shanghai Branch, CAS Center for Excellence and Synergetic Innovation Center in Quantum Information and Quantum Physics, University of Science and Technology of China, Shanghai 201315, China; [3]Shanghai Research Center for Quantum Sciences, Shanghai 201315, China; [4]Center for Quantum Information, Institute for Interdisciplinary Information Sciences, Tsinghua University, Beijing 100084, China and [5]Department of Materials, University of Oxford, Oxford OX1 3PH, UK

***Corresponding authors.** E-mails: xbzhu16@ustc.edu.cn; xma@tsinghua.edu.cn; yuaochen@ustc.edu.cn; pan@ustc.edu.cn
[†]Equally contributed to this work.

Received 6 August 2020; **Revised** 25 December 2020; **Accepted** 25 December 2020

ABSTRACT

Quantum error correction is an essential ingredient for universal quantum computing. Despite tremendous experimental efforts in the study of quantum error correction, to date, there has been no demonstration in the realisation of universal quantum error-correcting code, with the subsequent verification of all key features including the identification of an arbitrary physical error, the capability for transversal manipulation of the logical state and state decoding. To address this challenge, we experimentally realise the [5, 1, 3] code, the so-called smallest perfect code that permits corrections of generic single-qubit errors. In the experiment, having optimised the encoding circuit, we employ an array of superconducting qubits to realise the [5, 1, 3] code for several typical logical states including the magic state, an indispensable resource for realising non-Clifford gates. The encoded states are prepared with an average fidelity of 57.1(3)% while with a high fidelity of 98.6(1)% in the code space. Then, the arbitrary single-qubit errors introduced manually are identified by measuring the stabilisers. We further implement logical Pauli operations with a fidelity of 97.2(2)% within the code space. Finally, we realise the decoding circuit and recover the input state with an overall fidelity of 74.5(6)%, in total with 92 gates. Our work demonstrates each key aspect of the [5, 1, 3] code and verifies the viability of experimental realisation of quantum error-correcting codes with superconducting qubits.

Keywords: quantum error-correcting code, superconducting qubit, five-qubit code, error detection, logical operation

INTRODUCTION

Quantum computers can tackle classically intractable problems [1] and efficiently simulate many-body quantum systems [2]. However, quantum computers are notoriously difficult to control, due to their ubiquitous yet inevitable interaction with their environment, together with imperfect manipulations that constitute the algorithm. The theory of fault tolerance has been developed as the long-term solution to this issue, enabling universal error-free quantum computing with noisy quantum hardware [3–7]. The logical qubits of an algorithm can be represented using a larger number of flawed physical qubits. Providing that the machine is sufficiently large (high qubit count), and that physical errors happen with a probability below a certain threshold, then such errors can be systematically detected and corrected [8,9]. In experiment, several small quantum error-correcting codes (QECCs), including the repetition code [10–16], the four-qubit error-detecting code [17–19], the seven-qubit color code [20], the bosonic quantum error-correcting code [21,22] and others [23–26], have been realised with different hardware platforms. These works have shown the success of realising error-correcting codes with

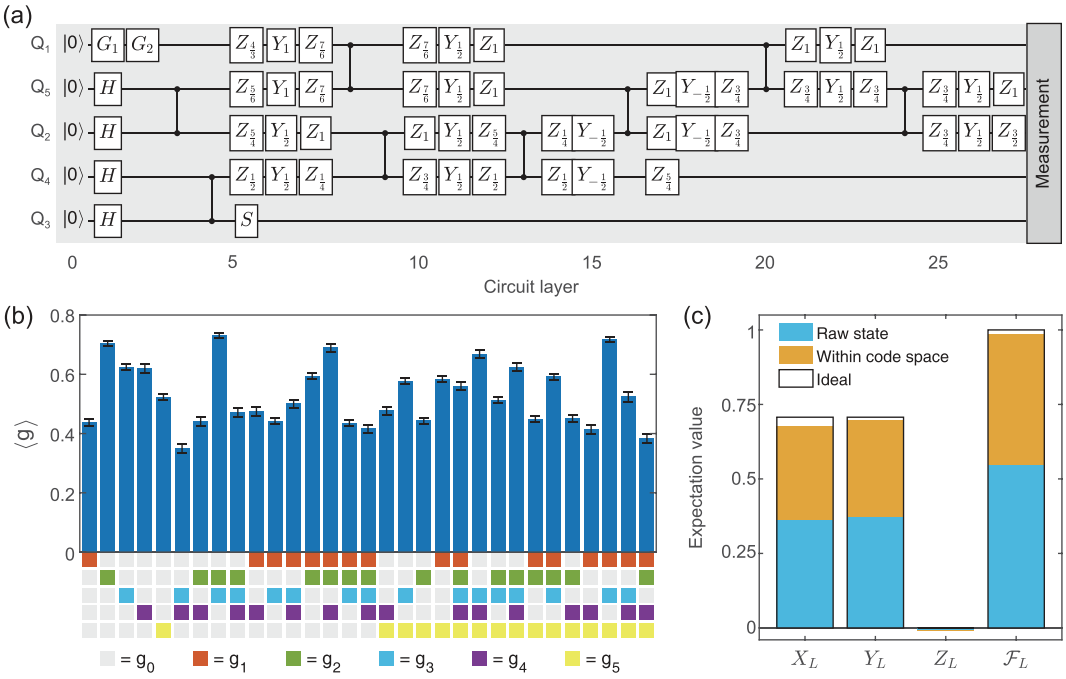

Figure 1. (a) Encoding quantum circuit of the five-qubit code. Here, the qubit labels $Q_1 \sim Q_5$ are arranged to correspond with Equation (1); G_1 and G_2 are single-qubit gates to prepare the input state $a\,|0\rangle + b\,|1\rangle$ for encoding; Y_α and Z_α are the rotation gates around the Y and Z axes for an angle $\alpha\pi$, respectively. In total, there are 27 layers of gate operations, including 54 single-qubit gates and eight nearest-neighbour controlled-phase gates. The single-qubit gates on different qubits can be applied in parallel, while the two-qubit gates can only be applied individually owing to the Z crosstalk. (b) Expectation values of 31 stabilisers for the encoded logical state $|T\rangle_L$. Error bars representing a 95% confidence interval are estimated via bootstrapping. (c) Expectation values of logical Pauli operators and state fidelity of the encoded magic state.

non-destructive stabiliser measurements and their application in extending the system lifetime [19,25]. Nevertheless, previous experiments are limited to restricted codes for correcting certain types of errors or the preparation of specific logical states. It remains an open challenge to realise a fully-functional QECC.

Here, we focus on the five-qubit [5, 1, 3] code, the 'perfect' code that can protect a logical qubit from an arbitrary single physical error using the smallest number of qubits [6,7]. While proof-of-principle experimental demonstrations of the [5, 1, 3] code have been conducted on NMR systems [27], whether it could be incorporated in more scalable quantum computing systems and protect errors presented in these systems remain open. Here, we focus on the realisation of the five-qubit code with superconducting qubit systems. As a preparatory theoretical step, we recompile the universal encoding circuit that prepares an arbitrary logical state in order to realise it with the fewest possible number of nearest-neighbour two-qubit gates. In experiment, we implement basic functions of the code by realising logical state preparation, transversal logical operations and state decoding.

THEORY

The five-qubit [5, 1, 3] code is a type of stabiliser code that is defined by a set of independent operators from the Pauli group, called stabilisers, such that the code space only has eigenvalue +1. The four stabilisers of the five-qubit code are

$$g_1 = X_1Z_2Z_3X_4I_5, \quad g_2 = I_1X_2Z_3Z_4X_5,$$
$$g_3 = X_1I_2X_3Z_4Z_5, \quad g_4 = Z_1X_2I_3X_4Z_5, \tag{1}$$

with I_i, X_i, Y_i, Z_i being the Pauli matrices acting on the ith qubit. The logical state space is defined by states $|\Psi\rangle_L = a\,|0\rangle_L + b\,|1\rangle_L$ that are simultaneously stabilised by the four stabilisers with $g_i\,|\Psi\rangle_L = +|\Psi\rangle_L$ for all $i = 1, 2, 3, 4$. Here, the logical states $|0\rangle_L$ and $|1\rangle_L$ are the basis states that are eigenstates of the logical Z_L operator. Any logical state $|\Psi\rangle_L$ can be uniquely determined by the four stabilisers defined in Equation (1) together with the fifth stabiliser $g_5 = |\Psi\rangle\langle\Psi|_L - |\Psi^\perp\rangle\langle\Psi^\perp|_L = (aa^* - bb^*)Z_L + (a^*b + b^*a)X_L - i(a^*b - b^*a)Y_L$, with $|\Psi^\perp\rangle = b^*\,|0_L\rangle - a^*\,|1_L\rangle$. That is, any logical state $|\Psi\rangle_L$ can be decomposed as

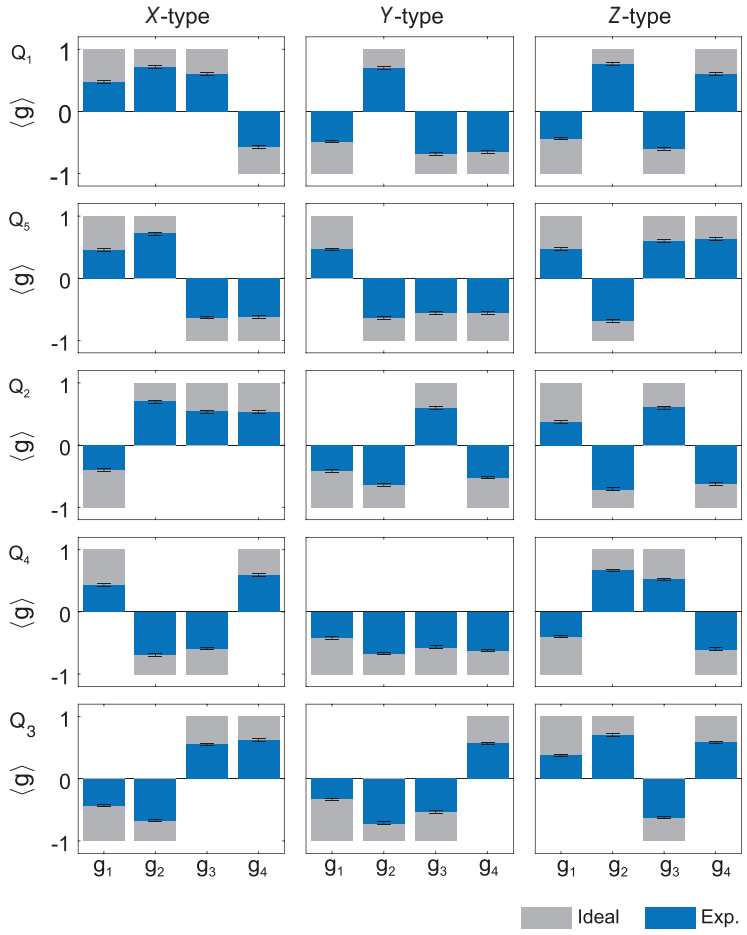

Figure 2. Destructive syndrome detection on the logic magic state $|T\rangle_L$. A single-qubit *X*-, *Z*- or *Y*-type error, which corresponds to a bit-flip, phase-flip or combined error, respectively, is applied to one of the five qubits Q_1 to Q_5. We destructively measure the four stabilisers and find consistent syndrome correlations that identify the quantum error.

$|\Psi\rangle_L \langle\Psi|_L = 2^{-5}\prod_{i=1}^{5}(g_0 + g_i)$, where $g_0 = I_1I_2I_3I_4I_5$ is the trivial stabiliser of all pure quantum states. Logical Pauli operators are transversely realised by applying the corresponding single-qubit gates on each physical qubit, $\sigma_L = \sigma_1\sigma_2\sigma_3\sigma_4\sigma_5$ for $\sigma = X, Y, Z$. General logical operators, such as the $T_L = e^{-iZ_L\pi/8}$ gate, may not be transversely realised.

The five-qubit code has distance three and therefore all single-qubit errors can be identified (and thus corrected) while all double-qubit errors can be detected. When there is no error, all stabiliser measurements should yield $+1$ for the encoded state $|\Psi\rangle_L$. When an error happens, one or more stabiliser measurements may yield -1. As there are four stabilisers whose measurement may take either $+1$ or -1 values, there are in total 15 syndrome measurement results with at least one outcome being -1. If we consider the ways in which a single Pauli error can afflict one of the five qubits, we note that there are 15 possibilities (three error types and five locations), with each mapping to a specific one of the 15 syndromes. When a two-qubit error happens, we again find that at least one of the stabiliser measurements takes -1. This heralds the fact that some error has occurred. However, since different double-qubit errors may have the same syndrome, we can only detect double-qubit errors without the capability of identifying or correcting them. Nevertheless, this latter property can be useful in some situations, such as state preparation, where we can simply discard a faulty realisation and restart.

Without using ancillary qubits, the original circuit for encoding the logical state $|\Psi\rangle_L$ requires a number of two-qubit gates that are non-local with respect to a linear architecture [6,7]. To tailor the circuit for superconducting systems that only involve nearest-neighbour controlled-phase gates, we recompile the encoding circuit to have the minimal possible number (eight) of nearest-neighbour control-phase gates as shown in Fig. 1(a). We provide the details of circuit compilation in the online supplementary material.

EXPERIMENTAL SETUP

The device for the implementation of the five-qubit error-correcting code is a 12-qubit superconducting quantum processor [28]. Among these 12 qubits, we chose five adjacent qubits to perform the experiment. The qubits are capacitively coupled to their nearest neighbours. The capacitively coupled *XY* control lines enable the application of single-qubit rotation gates by applying microwave pulses, and the inductively coupled *Z* control lines enable the double-qubit controlled-phase gates by adiabatically tuning the two-qubit state $|11\rangle$ close to the avoid level crossing of $|11\rangle$ and $|02\rangle$ [28]. After careful calibrations and gate optimisations, we have the average gate fidelities as high as 0.9993 for single-qubit gates and 0.986 for two-qubit gates. With the implementation of only single-qubit rotation gates and double-qubit controlled-phase gates, we realised the circuit for encoding and decoding of the logical state. More details about the experimental setup are given in the online supplementary material.

RESULTS

On a superconducting quantum processor [28], we experimentally realised the logical states $|0\rangle_L$, $|1\rangle_L$, $|\pm\rangle_L$ and $|\pm i\rangle_L$ that are eigenstates of the logical Pauli operators X_L, Y_L, Z_L and the magic state $|T\rangle_L = (|0\rangle_L + e^{i\pi/4}|1\rangle_L)/\sqrt{2}$ that cannot be realised by applying Clifford operations on any

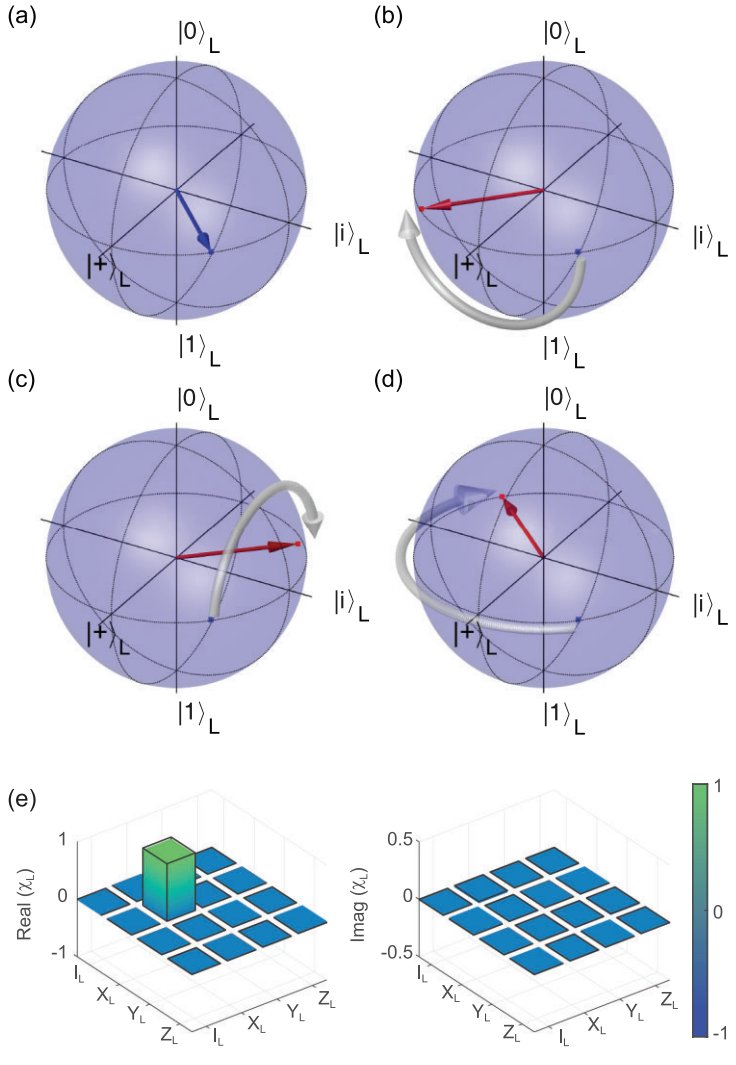

Figure 3. Logical operation within the code space. (a) Encoded logical state $|T\rangle_L$ illustrated on the logical Bloch sphere. (b)–(d) Single logical-qubit operation X_L, Y_L and Z_L applied on $|T\rangle_L$. The blue squares and vector are the initial states. The red circles and vectors are the final states. The states are projected into the code space. The fidelities of the state after gate operation are 98.6(1)%, 98.0(1)% and 98.7(1)% for (b), (c) and (d), respectively. The white arrow illustrates the dynamics under the gate operation. (e) The χ_L matrix of the logical X_L operation determined via quantum process tomography in the code space. The gate fidelity of logical X_L operation is determined to be 97.2(2)%. The black-outlined hollow bars correspond to the ideal X gate. We refer the reader to the online supplementary material for the definition of the χ_L matrix and details.

eigenstate of the logical Pauli operators. The expectation values of the stabiliser operators of $|T\rangle_L$ are shown in Fig. 1(b). The fidelity between the experimentally prepared state and the ideal state $|\Psi\rangle_L \langle\Psi|_L$ is determined by the measurement of the 32 stabiliser operators in $\prod_{i=1}^{5}(g_0 + g_i)$. We omit the g_0 one as it is constantly 1. In this way, we obtained the state fidelity as the average of the 32 stabilisers by picking up corresponding measurement results among the state tomography results. Finally, the state fidelity of $|T\rangle_L$ reaches 54.5(4)%. The fidelities of other prepared states are shown in the online supplementary material, with an average fidelity of 57.1(3)%. The main error in preparing the encoded state is from decoherence, especially the relatively short dephasing time. In a numerical simulation of the experiment with decoherence (see the online supplementary material for details), the state fidelity of $|T\rangle_L$ is 58.9%. After numerically increasing the dephasing time to be the same as the energy relaxation time, the state fidelity can be increased to 92.1%, indicating a potential direction for future improvements.

The quality of the prepared logical states can also be divided into its overlap with the logical code space and its agreement with the target logical state after projecting it into the code space. Given the logical Pauli operators X_L, Y_L, Z_L and $I_L = |0\rangle_L \langle 0|_L + |1\rangle_L \langle 1|_L$, the normalised density matrix ρ_L is defined by projecting the experimentally prepared state ρ_q into the code space

$$\rho_L = \frac{I + \tilde{P}_X X_L + \tilde{P}_Y Y_L + \tilde{P}_Z Z_L}{2}, \qquad (2)$$

with normalised probability $\tilde{P}_j = P_j / P_I$ and $P_j = \mathrm{Tr}(\rho_q \sigma_L)$ for all $\sigma = I, X, Y, Z$, where ρ_q is the density matrix of the five-qubit state. We define the fidelity within the code space by $\mathcal{F}_L = \langle\Psi|_L \rho_L |\Psi\rangle_L$, as shown in Fig. 1(c), with the average value being as high as 98.6(1)%. Since projecting to the code space is equivalent to post-selecting all +1 stabiliser measurements, our result also indicates the possibility of high-fidelity logical state preparation with future non-destructive stabiliser measurements. This relies on whether we can achieve accurate non-destructive stabiliser measurements, especially whether errors from the ancillary qubits and additional gates are sufficiently low.

Given the realisation of the logical state, one can proceed to verification of the error correction/detection ability of the five-qubit code. Acting on the logical encoded state $|T\rangle_L$, we systematically introduce every type of single-qubit error by artificially applying the corresponding single-qubit gate on one of the five qubits. Then, by measuring the four stabilisers g_1, g_2, g_3 and g_4, we aim to verify that each error would be properly identified. As shown in Fig. 2(a), for each case, we do indeed find the corresponding syndrome pattern that identifies the location of the single-qubit error. Suppose that the expectation value of ith stabiliser is p_i; then the probability that the syndrome measurement works is $\prod_i (|p_i| + 1)/2$, which is 0.413 on average in experiment. We also apply double-qubit errors on $|T\rangle_L$

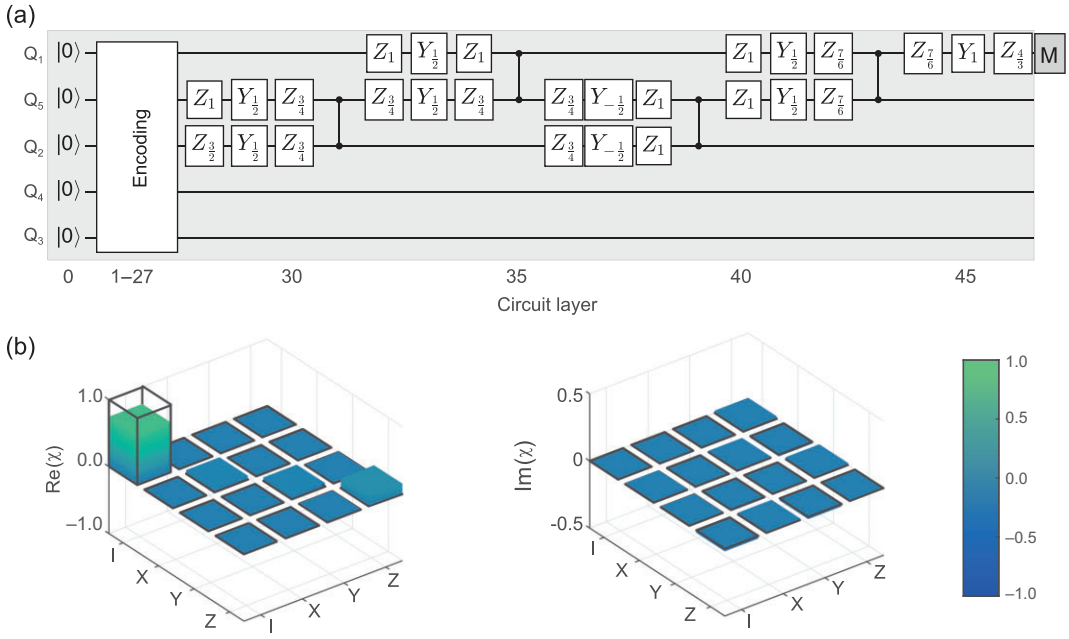

Figure 4. Decoding of the five-qubit code. (a) Decoding quantum circuit. After the logical state prepared with the encoding circuit shown in Fig. 1(b), we apply the decoding circuit to map the state back to a single-qubit state. The decoding circuit is essentially a reverse encoding circuit, except the gates applied on Q_3 and Q_4 are omitted because they do not affect the final decoded qubit. (b) The χ_L matrix of the encoding and decoding circuits. The color bars are the experimental χ_L matrix and the black-outlined hollow bars correspond to the identical process. The process fidelity reaches 74.5(6)%.

and find the same syndrome correlation that can always detect the existence of errors (see the online supplementary material for details). Notably, the (single-qubit or double-qubit) error-afflicted states have probabilities projecting onto the code space (around 3.3%), verifying the power of the error-correcting code.

In a functioning fault-tolerant quantum computer, operations on logical qubits are realised through a series of operations on the component physical qubits. We implement and verify three such transversal logical operations. Starting from the magic state $|T\rangle_L$ presented in Fig. 3(a), we demonstrate the single logical-qubit operations X_L, Y_L and Z_L and plot the rotated states within the code space, as shown in Fig. 3(b), (c) and (d), respectively. To characterise these logical operations, we performed the quantum process tomography within the code space as shown in Fig. 3(e), which reflects how well logical operations manipulate logical states. We determine gate fidelities of the logical X_L, Y_L and Z_L operations to be 97.2(2)%, 97.8(2)% and 97.3(2)%, respectively.

Finally, after encoding the single-qubit input state into the logical state, we apply the decoding circuit, see Fig. 4(a), to map it back to the input state. With input states $|0\rangle$, $|1\rangle$, $|+\rangle$, and $|+i\rangle$, we determine the state fidelity after decoding as 87.4(5)%, 91.6(4)%, 76.7(6)%, and 77.1(6)%, respectively. The relatively lower fidelities for $|+\rangle$ and $|+i\rangle$ states are also caused by the short dephasing time. After quantum process tomography from the four output states, the process fidelity is determined as 74.5(6)%, as shown in Fig. 4(b). The decoding circuit only applies operations on three qubits, highlighting the ability of quantum secret sharing with the five-qubit code [29]. This simplification is due to a consequence of locality: no observable on Q_1 can be affected by the omitted independent gate operations of the other qubits.

DISCUSSION

An essential milestone on the road to fault-tolerant quantum computing is the achievement of error-corrected logical qubits that genuinely benefit from error correction, outperforming simple physical qubits. There are three steps for achieving this goal: (1) realising encoded logical qubits in a code capable of detecting and correcting errors, (2) realising operations on encoded qubits and error-correction cycles and (3) adding more ancillary qubits and improving the operation fidelity to achieve fault tolerance. Our experiment completes step (1) by realising the basic ingredients of the full functional five-qubit error-correcting code. Our work partially achieves step (2) as we indeed perform logical operations and verify error detection; however, because we are only able to evaluate stabilisers destructively, we cannot perform full error correction. Directions for future

works include the realisation of non-destructive error detection [25,26,30] and error correction, and the implementation of logical operations on multiple logical qubits for the five-qubit code. Our work also has applications in error mitigation for near-term quantum computing [31].

DATA AVAILABILITY

All data analysed to evaluate the conclusions are available from the authors upon reasonable request.

SUPPLEMENTARY DATA

Supplementary data are available at *NSR* online.

ACKNOWLEDGEMENTS

The authors thank the USTC Center for Micro- and Nanoscale Research and Fabrication, Institute of Physics CAS and National Center for Nanoscience and Technology for supporting the sample fabrication. The authors also thank QuantumCTek Co., Ltd. for supporting the fabrication and maintenance of room-temperature electronics.

FUNDING

This work was supported by the National Key Research and Development Program of China (2017YFA0304300, 2017YFA0303900 and 2017YFA0304004), the National Natural Science Foundation of China (11875173, 11674193, 11574380 and 11905217), the Chinese Academy of Sciences, the Science and Technology Committee of Shanghai Municipality (16DZ2260100), the Anhui Initiative in Quantum Information Technologies, and the Engineering and Physical Sciences Research Council (EP/M013243/1 to S.C.B and X.Y.).

AUTHOR CONTRIBUTIONS

X.M., Y.-A.C., X.-B.Z. and J.-W.P. conceived the research. M.G., X.Y., X.M. and X.-B.Z. designed the experiment. S.-Y.W. designed the sample. H.D. and H.R. prepared the sample. X.Y., Z.Z., Q.Z., Y.-C.L. and H.L. designed the quantum circuit. M.G., Y.-L.W., Y.-W.Z., C.Z. and S.-W.L. carried out the experiments. Y.-L.W. developed the programming platform for measurements. M.G., X.Y., Y.-W.Z., C.Z., S.B., X.M., Y.-A.C. and X.-B.Z. analysed the results. F.-T.L., J.L., Y.X. and C.-Z.P. developed room-temperature electronics equipment. All authors contributed to discussions of the results and development of the manuscript. X.-B.Z. and J.-W.P. supervised the whole project.

Conflict of interest statement. None declared.

REFERENCES

1. Shor PW. Algorithms for quantum computation: discrete logarithms and factoring. In: *Proceedings 35th Annual Symposium on Foundations of Computer Science*. Los Alamitos, CA: IEEE Computer Society Press, 1994, 124–34.
2. Lloyd S. Universal quantum simulators. *Science* 1996; **273**: 1073–8.
3. Gottesman D. Theory of fault-tolerant quantum computation. *Phys Rev A* 1998; **57**: 127–37.
4. Shor PW. Scheme for reducing decoherence in quantum computer memory. *Phys Rev A* 1995; **52**: R2493–6.
5. Steane AM. Error correcting codes in quantum theory. *Phys Rev Lett* 1996; **77**: 793–7.
6. Bennett CH, DiVincenzo DP and Smolin JA *et al.* Mixed-state entanglement and quantum error correction. *Phys Rev A* 1996; **54**: 3824–51.
7. Laflamme R, Miquel C and Paz JP *et al.* Perfect quantum error correcting code. *Phys Rev Lett* 1996; **77**: 198–201.
8. Knill E. Quantum computing with realistically noisy devices. *Nature* 2005; **434**: 39–44.
9. Aliferis P, Gottesman D and Preskill J. Quantum accuracy threshold for concatenated distance-3 codes. *Quantum Info Comput* 2006; **6**: 97–165.
10. Chiaverini J, Leibfried D and Schaetz T *et al.* Realization of quantum error correction. *Nature* 2004; **432**: 602–5.
11. Schindler P, Barreiro JT and Monz T *et al.* Experimental repetitive quantum error correction. *Science* 2011; **332**: 1059–61.
12. Reed MD, DiCarlo L and Nigg SE *et al.* Realization of three-qubit quantum error correction with superconducting circuits. *Nature* 2012; **482**: 382–5.
13. Waldherr G, Wang Y and Zaiser S *et al.* Quantum error correction in a solid-state hybrid spin register. *Nature* 2014; **506**: 204–7.
14. Riste D, Poletto S and Huang MZ *et al.* Detecting bit-flip errors in a logical qubit using stabilizer measurements. *Nat Commun* 2015; **6**: 6983.
15. Cramer J, Kalb N and Rol MA *et al.* Repeated quantum error correction on a continuously encoded qubit by real-time feedback. *Nat Commun* 2016; **7**: 11526.
16. Wootton JR and Loss D. Repetition code of 15 qubits. *Phys Rev A* 2018; **97**: 052313.
17. Lu CY, Gao WB and Zhang J *et al.* Experimental quantum coding against qubit loss error. *Proc Natl Acad Sci USA* 2008; **105**: 11050–4.
18. Bell B, Herrera-Martí D and Tame M *et al.* Experimental demonstration of a graph state quantum error-correction code. *Nat Commun* 2014; **5**: 3658.
19. Linke NM, Gutierrez M and Landsman KA *et al.* Fault-tolerant quantum error detection. *Sci Adv* 2017; **3**: e1701074.
20. Nigg D, Mueller M and Martinez EA *et al.* Quantum computations on a topologically encoded qubit. *Science* 2014; **345**: 302–5.
21. Ofek N, Petrenko A and Heeres R *et al.* Extending the lifetime of a quantum bit with error correction in superconducting circuits. *Nature* 2016; **536**: 441–5.
22. Campagne-Ibarcq P, Eickbusch A and Touzard S *et al.* Quantum error correction of a qubit encoded in grid states of an oscillator. *Nature* 2020; **584**: 368–72.

23. Yao XC, Wang TX and Chen HZ *et al*. Experimental demonstration of topological error correction. *Nature* 2012; **482**: 489–94.
24. Taminiau TH, Cramer J and Sar T *et al*. Universal control and error correction in multi-qubit spin registers in diamond. *Nat Nanotechnol* 2014; **9**: 171–6.
25. Kelly J, Barends R and Fowler AG *et al*. State preservation by repetitive error detection in a superconducting quantum circuit. *Nature* 2015; **519**: 66–9.
26. Andersen CK, Remm A and Lazar S *et al*. Repeated quantum error detection in a surface code. *Nat Phys* 2020; **16**: 875–80.
27. Cory DG, Price MD and Maas W *et al*. Experimental quantum error correction. *Phys Rev Lett* 1998; **81**: 2152–5.
28. Gong M, Chen MC and Zheng Y *et al*. Genuine 12-qubit entanglement on a superconducting quantum processor. *Phys Rev Lett* 2019; **122**: 110501.
29. Cleve R, Gottesman D and Lo HK. How to share a quantum secret. *Phys Rev Lett* 1999; **83**: 648–51.
30. Bultink CC, O'Brien TE and Vollmer R *et al*. Protecting quantum entanglement from leakage and qubit errors via repetitive parity measurements. *Sci Adv* 2020; **6**: eaay3050.
31. McClean JR, Jiang Z and Rubin NC *et al*. Decoding quantum errors with subspace expansions. *Nat Commun* 2020; **11**: 636.